Published in final edited form as:
J Invest Dermatol. 2015 November ; 135(11): 2842–2851. doi:10.1038/jid.2015.224.

Ultrasonic stimulation of mouse skin reverses the healing delays in diabetes and aging by activation of Rac1

James A Roper[1], **Rosalind C Williamson**[1], **Blandine Bally**[1], **Christopher AM Cowell**[1], **Rebecca Brooks**[1], **Phil Stephens**[2], **Andrew J Harrison**[3], and **Mark D Bass**[1,4,*]

[1]School of Biochemistry, University of Bristol, University Walk, Bristol, BS8 1TD, United Kingdom

[2]Wound Biology Group, Cardiff Institute of Tissue Engineering and Repair, School of Dentistry, College of Biomedical and Life Sciences, Cardiff University, Heath Park, Cardiff, CF14 4XY, Wales, United Kingdom

[3]Bioventus LLC, 4721 Emperor Boulevard, Suite 100, Durham, NC 27703, USA

[4]Centre for Membrane Interactions and Dynamics, Department of Biomedical Science, University of Sheffield, Western Bank, Sheffield, S10 2TN, United Kingdom

Abstract

Chronic skin healing defects are one of the leading challenges to lifelong wellbeing, affecting 2-5% of populations. Chronic wound formation is linked to age and diabetes and frequently leads to major limb amputation. Here we identify a strategy to reverse fibroblast senescence and improve healing rates. In healthy skin, fibronectin activates Rac1 in fibroblasts, causing migration into the wound bed and driving wound contraction. We discover that mechanical stimulation of skin with ultrasound can overturn healing defects by activating a calcium/CamKinaseII/Tiam1/Rac1 pathway that substitutes for fibronectin-dependent signaling and promotes fibroblast migration. Treatment of diabetic and aged mice recruits fibroblasts to the wound bed and reduces healing times by 30%, restoring healing rates to those observed in young, healthy animals. Ultrasound treatment is equally effective in rescuing the healing defects of animals lacking fibronectin receptors, and can be blocked by pharmacological inhibition of the CamKinaseII pathway. Finally, we discover that the migration defects of fibroblasts from human venous leg ulcer patients can be reversed by ultrasound, demonstrating that the approach is applicable to human chronic samples. By demonstrating that this alternative Rac1 pathway can substitute for that normally operating in skin, we identify future opportunities for management of chronic wounds.

Keywords

Ultrasound; Healing; Diabetes; Age; Rac1

*Correspondence: mark.bass@sheffield.ac.uk, Tel: +44 114 222 5278, ORCID: 0000-0002-8854-9705.

Conflict of Interest: Andrew Harrison is an employee of Bioventus LLC.

Europe PMC Funders Author Manuscripts

Introduction

Chronic healing defects are one of the largest current health challenges, affecting over 6.5 million patients in the US and costing over US$25 billion annually (Sen *et al.*, 2009). The major risk factors are diabetes, age, obesity and smoking (Galiano and Mustoe, 2007; Sen *et al.*, 2009), meaning that the challenge of treating chronic wounds is escalating as the risk factors become more common. Current approaches to wound treatment such as debridement and antibiotic treatment to reduce infection and pressure treatment to increase blood flow are effective in some, but not all cases. Topical application of growth factors to activate cells has been disappointing due to the abundance of proteolytic enzymes in a chronic wound and while injection of mesenchymal stem cells or modified fibroblasts is effective, it is prohibitively expensive (Woodley *et al.*, 2007; Zahorec *et al.*, 2014). Therefore it is important that we discover ways to manipulate cell types already *in situ*. Acute wound closure can be divided into four main processes: inflammation, fibroblast-dependent wound contraction, re-epithelialisation and angiogenesis (Shaw and Martin, 2009). Delays in the healing of acute wounds leads to the formation of chronic wounds and examination of the cellular defects of chronic wounds highlights a chronic inflammatory response and fibroblast senescence as the two key defects (Harding *et al.*, 2005; Menke *et al.*, 2007; Wall *et al.*, 2008). While current wound therapy focuses on management of bacterial burden and the inflammatory response, effective strategies for manipulating the fibroblast population are still lacking (Galiano and Mustoe, 2007).

Upon wounding, fibronectin deposited by macrophages or leaking from damaged blood vessels (Shaw and Martin, 2009) engages α5β1-integrin and syndecan-4 on the surface of fibroblasts, activating the Rac1 pro-migratory signal (Bass *et al.*, 2007). Knockout of syndecan-4 or fibroblast-specific knockout of Rac1 retard wound closure (Echtermeyer *et al.*, 2001; Liu *et al.*, 2009), whereas topical application of fibronectin or overexpression of constitutively active Rac1 accelerates cutaneous repair (Hassanain *et al.*, 2005; Kwon *et al.*, 2007). Rac1 plays a central role in most cell migration processes and can be activated by a large number of guanine-nucleotide-exchange factors (GEFs) downstream of a number of signaling pathways (Raftopoulou and Hall, 2004). The range of regulatory mechanisms means that it may be possible to activate Rac1 in skin fibroblasts and drive migration by pathways other than the fibronectin-dependent route. One possibility is to use mechanical, rather than chemical stimuli to activate Rac1. Indeed, stimulation of cultured fibroblasts with ultrasound activates Rac1 by a syndecan-4-independent mechanism (Mahoney *et al.*, 2009). Interestingly, clinical trials have revealed that ultrasound accelerates fracture repair by 30-40% (Heckman *et al.*, 1994; Kristiansen *et al.*, 1997) by promoting endochondral ossification (Azuma *et al.*, 2001; Leung *et al.*, 2004), and this approach has received approval for clinical fracture therapy from the FDA (US Food and Drug Administration) in 1994 and NICE (UK National Institute for Health and Care Excellence) in 2013. However the possibility that ultrasound might also accelerate soft tissue repair has not been investigated.

In this study, we identify a mechanism of Rac1 activation that can substitute for the fibronectin-dependent pathway that operates in healing of healthy skin. We demonstrate that activation of the pathway by mechanical stimulation, with ultrasound, rescues healing

defects caused by diabetes, age or defects in fibronectin signaling by enhancing wound fibroblast migration. We go on to show that such treatments have similar effects on patient chronic wound fibroblasts, indicating that such approaches could be efficacious in clinical situations.

Results & Discussion

Acceleration of dermal repair in impaired healing models

To examine the effect of mechanical stimuli on dermal wound closure, we compared the effect of a 20-minute daily ultrasound treatment, proven to be efficacious for fracture repair (30 $mWcm^{-2}$, 1.5 MHz wave frequency, 1 kHz pulse frequency), with a sham treatment where the device was applied, but not activated. In the absence of a true chronic wound animal model, diabetic mice are the most commonly used impaired healing murine model (Ansell *et al.*, 2012). Non-obese diabetic (NOD) mice, which spontaneously develop type-1 diabetes (Atkinson and Leiter, 1999) suffered a delay in the closure of 4-mm full-thickness skin punch wounds, compared to non-diabetic mice (Fig. 1A). Wound size was significantly reduced at days 6 and 7 in diabetic mice that received ultrasound treatment (Fig. 1A+B) and treatment reduced the wound resolution time, at which the scab fell off, from 9 to 6 days (Fig. 1C). Therefore, ultrasound stimulation reduced healing times by 33% and restored the healing mechanisms of diabetic animals to those observed in healthy controls. Age is a second key risk factor in poor healing prognosis. The effect on 18-month-old mice was even more pronounced, with significant healing retardation of untreated mice at days 3-9, compared with 3-month-old or ultrasound-treated 18-month-old mice (Fig. 1D-E). Again, ultrasound reduced the wound resolution time from 9 to 6 days (Fig.1F). These results clearly demonstrate that daily ultrasound treatment assists wound closure in terms of both wound size, and the time taken for wounds to resolve to levels indistinguishable from young mice.

The effect of ultrasound on wound area caused us to examine the effect on early wound responses, namely inflammation and wound contraction by fibroblasts. Ultrasound treatment increased the number of fibroblast specific protein (FSP) positive fibroblast cells at the wound shoulder at 72 hours post-wounding (Fig. 1G-H, Supplementary Fig. 1A-B), whilst F4/80 staining of macrophages (Fig. 1I-J, Supplementary Fig. 1C-D) or fibronectin deposition (Supplementary Fig. 1E) were unaffected by ultrasound. Therefore, we conclude that ultrasound restores healing to diabetic and aged animals by activating fibroblasts. The finding fits with our clinical understanding of defective healing in diabetes, which has been attributed to fibroblast senescence and loss of migratory response, as well as neuropathy and ischemia (Falanga, 2005). These findings caused us to look more closely at the effect of ultrasound on fibroblast behavior.

Fibroblast migration is guided by engagement of the fibronectin receptors, $\alpha5\beta1$-integrin and syndecan-4, which leads to activation of the protrusive signal, Rac1, and is required for efficient wound closure (Bass *et al.*, 2007; Echtermeyer *et al.*, 2001; Liu *et al.*, 2009). We have previously demonstrated that ultrasound activates Rac1 in syndecan-4-null fibroblasts and drives linear migration in the absence of a fibronectin guidance cue (Mahoney *et al.*, 2009). Therefore we examined whether ultrasound can rescue the healing defects of *Sdc4* -/-

mice. *Sdc4* -/- mice suffer a healing delay compared to wild-type, although it is not as severe as that of the diabetic and aged mice (Fig. 1K). Ultrasound treatment accelerated wound closure rate and reduced resolution time of *Sdc4* -/- mice (Fig. 1K-M) and specifically drove recruitment of fibroblasts (Fig. 1N, Supplementary Fig. 2A+B). By contrast, ultrasound had no effect on wild-type animals, which already healed efficiently (Supplementary Fig. 2C-G). Taken together, we demonstrate that the mechanical ultrasound stimulus activates fibroblasts and overcomes wound-healing defects in both pathological and specific knockout mouse models.

Ultrasound induces persistent migration

In the dermis, collagen and fibronectin are arranged into aligned fibres that act as guidance cues and cause linear migration of fibroblasts. An *in vitro* approximation of this matrix structure can be generated by lysing fibroblasts from a cultured monolayer to yield exposed cell-derived matrix (CDM). CDM allows detailed analysis of ability of individual migrating cells to follow fibers, and migration persistence can be calculated by dividing linear displacement of a cell by total distance moved. Wild-type cells migrate persistently over CDM, whereas *Sdc4* -/- fibroblasts migrate randomly, due to dysregulated Rac1 signaling (Bass *et al.*, 2007). Ultrasound stimulation of wild-type fibroblasts had no effect on speed, and did not significantly increase the persistence, as wild-type fibroblasts already exhibit linear migration (Fig. 2A-C, Supplementary Movie 1). Although ultrasound did not affect the speed of *Sdc4* -/- fibroblasts, it caused the cells to switch from random to persistent migration (Fig. 2D-F), consistent with the recruitment of fibroblasts to the wound shoulder seen *in vivo* (Fig. 1M + Supplementary Fig. 2A). To test whether the migration effect is applicable to human chronic wound samples, we repeated the experiment using senescent-like fibroblasts isolated from the chronic venous leg ulcer (VLU) of a 71-year old female patient with wound duration of greater than 7 months. With the VLU fibroblasts, the effect of ultrasound was even more dramatic than *Sdc4* -/- fibroblasts, increasing both the speed and persistence of migration (Fig. 2G-I, Supplementary Movie 2). The increase in severity of the migration defect of the chronic sample compared to the *Sdc4* -/- sample matches the greater effect on healing seen with aged or diabetic mice, compared to *Sdc4* -/-. Importantly, these results show that although pathological defects are more severe than simple knockout models, ultrasound is capable of reactivating fibroblasts and restoring both, so is broadly applicable.

Alternative Rac1 Activation Mechanisms

We know that Rac1 activation is a key event in skin repair, and that engagement of syndecan-4 by fibronectin activates Rac1 in healthy skin fibroblasts. We also know that ultrasound negates the need for syndecan-4 in wound healing, and so we tested whether ultrasound was activating Rac1 by an alternative pathway. Rac1 is activated by exchange of bound GDP for GTP, governed by the activity of guanine-nucleotide exchange factors (GEFs) (Raftopoulou and Hall, 2004), and so we tested the role of a number of GEFs in mediating the ultrasound signal, using effector pull-down assays. Ultrasound elicited a wave of Rac1 activity in control knockdown MEFs (Fig. 3A). Reducing the ultrasound intensity attenuated the 30-minute peak in Rac1 activity, confirming that the Rac1 response was indeed a consequence of the ultrasound wave (Supplementary Fig. 3A). Rac1 activation was

not blocked by RNAi of Rac-GEFs, Vav2 or Dock180 (Fig. 3B-C, F). By contrast, Rac1 activation was ablated in *Tiam1* -/- MEFs, and could be rescued by re-expression of Tiam1 (Fig. 3D-F). To ensure that ultrasound stimulation was coupled to signaling downstream of Rac1, phosphorylation of p21 activated kinase 1 (PAK) was measured be in-cell ELISA. Ultrasound induced PAK phosphorylation that was blocked by knockout of Tiam1, but not knockdown of other GEFs (Fig. 3G-K). Finally, specificity of the ultrasound signal was tested by examining the related GTPase, Cdc42. Ultrasound had no effect on Cdc42 activity (Supplementary Fig. 3B), demonstrating a specific effect on Rac1.

CaMKII mediates the ultrasound response

Tiam1 is activated by phosphorylation by protein kinase C (PKC) and calmodulin kinase II (CaMKII) (Fleming *et al.*, 1999). We have previously reported that ultrasound functions independently of PKC (Mahoney *et al.*, 2009), and so we investigated the role of CaMKII. Inhibition of CaMKII activity with the pharmacological inhibitor, KN93, or siRNA blocked PAK phosphorylation upon ultrasound stimulation (Fig. 4A-C). Furthermore, ultrasound triggered activating autophosphorylation of CamKII (Thr286) demonstrating that CamKII mediates the ultrasound effect (Fig. 4D).

CaMKII is itself activated by association with calcium-bound calmodulin (Swulius and Waxham, 2008), leading us to test whether calcium levels affected the ultrasound response. Disruption of the intracellular calcium stores (thapsigargin), chelation of extracellular calcium (BAPTA) or chelation of all calcium (membrane permeable, BAPTA-AM) each blocked PAK phosphorylation in response to ultrasound, demonstrating that calcium flux plays a key role in mediating the ultrasound signal (Fig. 4E). Crucially, thapsigargin and BAPTA had no effect on PAK-phosphorylation in response to fibronectin fragments (Fig. 4F), demonstrating that the cells were still capable of mounting a response and that ultrasound and fibronectin activate Rac1 by separate pathways. Collectively, these experiments identify a calcium-dependent pathway of Rac1 activation that is independent of the fibronectin-triggered pathway that occurs in healthy fibroblasts (Fig. 4G).

Healing signals converge on Rac1

We propose that ultrasound-triggered signals and normal wound signals converge on the key migration regulator, Rac1, explaining how ultrasound can rescue wound healing defects arising from a number of situations. We tested the hypothesis by blocking the ultrasound-triggered pathway in our mouse models. Application of the pharmacological Rac1 inhibitor, EHT 1864, to wounds on wild-type mice severely retarded wound contraction and furthermore blocked the ability of ultrasound to rescue healing, demonstrating that normal and ultrasound-induced pathways converge on Rac1 (Fig. 5A). Fibronectin-dependent and ultrasound-dependent pathways were tested using a combination of syndecan-4 knockdown and pharmacological inhibition of CamKII with KN93. KN93 had no effect on wound closure in wild-type mice where fibronectin signaling was intact (Fig. 5B). However, in *Sdc4* -/- mice where fibronectin signaling is perturbed, KN93 blocked the ability of ultrasound to rescue normal wound closure (Fig. 5C). These results demonstrate that Rac1 activation is crucial for efficient wound closure, but that it can be achieved in different ways. In the

Europe PMC Funders Author Manuscripts

absence of signaling through syndecan-4, stimulation of a CamKII pathway is a viable route for Rac1 activation and ultrasound treatment provides a robust mechanism for doing that.

Collectively our experiments demonstrate that Rac1 can be activated in wound fibroblasts using a mechanical, ultrasound stimulus. This calcium-CamKII-Tiam1-mediated pathway can substitute for the fibronectin triggered pathway seen during the healing of healthy skin and restores normal healing to a number of pathological healing mouse models.

Comparison to the fracture-repair registry

The standout discovery in this manuscript is that healing times in diabetic or aged mice can be reduced by 33% (Fig. 1), which is comparable with the 30-40% reduction in healing times of tibial and radial fractures (Heckman *et al.*, 1994; Kristiansen *et al.*, 1997). The similarity is surprising as the mechanisms differ. We demonstrate that in skin healing, ultrasound stimulates Rac1 signalling and fibroblast migration, but has no effect on macrophage recruitment. By contrast, ultrasound in fracture repair has been linked to inflammatory signals and induces COX-2 expression and prostaglandin E2 secretion (Tang *et al.*, 2006), resulting in differentiation of mesenchymal cells into osteoblasts and chondrocytes that leads to endochrondal ossification (Pounder and Harrison, 2008). Nevertheless, the rescue of skin healing that we report matches the reported restoration of delayed fracture healing caused by diabetes (Coords *et al.*, 2011) or age (Naruse *et al.*, 2010) in rodents. A second feature of our findings is that ultrasound has limited effect on the healing rates of young healthy mice, which already heal efficiently (Fig. S2C+D). Registry studies of clinical investigations into the use of ultrasound for fracture repair have revealed similar trends. While the clinical study by Heckman *et al.* demonstrated that ultrasound accelerated fracture healing in patients by 38% (Heckman *et al.*, 1994), another study that excluded risk factors such as smoking and alcohol from the study group did not find a significant effect of ultrasound on fracture repair (Emami *et al.*, 1999). The similarities between groups that benefit from ultrasound treatment during fracture and skin repair are encouraging as inspection of a large FDA-reviewed registry of non-union fractures treated with ultrasound reveals that although untreated fractures heal 63-87% less efficiently in diabetic than healthy patients, ultrasound induced closure of non-unions in 82% (71/87) of diabetics, similar to the 83% (1283/1546) closure rate observed across the entire registry (Frankel and Mizuho, 2002). If, as our findings suggest, the beneficial effect of ultrasound can be extrapolated from fracture to skin healing, then a solution to treatment of chronic wounds would be within our grasp.

An issue that has hindered the clinical use of ultrasound is that different studies have used a range of ultrasound parameters with a range of success. Efficacy in fracture repair has been demonstrated using ultrasound intensities ranging from 2 mW/cm^2 to 500 mW/cm^2 (Angle *et al.*, 2011; Claes and Willie, 2007) although intensities above 100 mW/cm^2 have been reported to result in lower maximum torque in the repaired bone than intensities of 30-50 mW/cm^2 (Claes and Willie, 2007). Previous studies into effects on skin healing have been even more diverse, with most studies examining low-frequency ultrasound as a form of physiotherapy massage. One study using high frequency (3 MHz) ultrasound actually found that treatment retarded healing of ischemic skin flap wounds in rats (Altomare *et al.*, 2009)

but this study applied ultrasound at 500 mW/cm^2. At below 50 mW/cm^2 the thermal effects of ultrasound are negligible (0.01°C (Duarte, 1983)), but at 500 mW/cm^2 would be sufficient to affect temperature-sensitive enzymes such as matrix metalloproteinases and collagenase (Claes and Willie, 2007). It is logical that an ischemic wound would be more susceptible to such damage, due to the reduced ability to dissipate heat.

In this study, we find that reduction of ultrasound intensity attenuates Rac1 activation in fibroblasts (Supplementary figure 3A). By contrast, signals as low as 2 mW/cm^2 have been reported to be sufficient to trigger differentiation and mineralisation of bone marrow stromal cells (Angle *et al.*, 2011). One possible explanation would be that molecular mechanisms differ between bone and skin healing, but a second would be that a threshold of active Rac1 is required to activate a cell, and that 2 mW/cm^2 is sufficient to reach that threshold in stromal cells. Indeed, we previously reported that the threshold for focal adhesion-formation by fibroblasts is 20-25 mW/cm^2 (Mahoney *et al.*, 2009). The threshold differences between cell types mean that the ultrasound dose needs to be optimised, and is even more complicated *in vivo*. Ultrasound is attenuated as it passes through tissue, and then reflected at the bone-soft tissue interface (Claes and Willie, 2007). Such effects mean that the same emitter delivers different intensities of ultrasound at a skin compared to a fracture, and it is probable that the optimal regimes for treating fractures and skin wounds will differ. Therefore, our current findings represent the first step towards skin healing therapy and there is now great scope and great need for refinement, to develop the optimal therapeutic regimes for both skin and bone treatments.

Materials & Methods

Animals

Animal experiments were performed in accordance with Home Office regulations described by the UK Animals (Scientific Procedures) Act 1986, UK project license 30/2791. Syndecan-4 wild-type and knockout C57BL/6J mice (Ishiguro *et al.*, 2000) generated by heterozygous (*Sdc4* (+/-) C57BL/6J) parental crosses were used at age 12 weeks for comparison of genotypes. Wild-type mice were used at 18 months for the ageing study. Male NOD mice were maintained in a clean environment to maximize spontaneous diabetes development. Onset of diabetes was monitored weekly prior to experiments by urine glucose measurements (Diastix, Bayer), and daily thereafter until sacrifice.

Punch wound experiments

Mice were anaesthetized by isofluorane inhalation for initial wounding and daily treatment with ultrasound. To create wounds, two pairs of full-thickness 4mm excisional punch wounds were made either side of the dorsal midline of the barbered back of each animal. Wound size was recorded by photographing mice at the same time each day prior to treatment. Where relevant, rate constants of curves were calculated by fitting a one-phase decay with GraphPad Prism. For application of drugs, 30% pluronic gel (Sigma) with and without 50μM EHT1864 (Sigma) or 20μM KN93 (Calbiochem) was maintained as a liquid at 4°C before it was administered directly to the wound by pipette immediately after wounding and allowed to solidify.

Ultrasound stimulation

Mouse wounds or cells in culture were coupled to 2.5-cm diameter ultrasound transducer (Exogen; Bioventus LLC, Durham, NC) using water-based gel (Exogen). During stimulation experiments, the transducer generated 30 mW/cm^2 (spatial average, temporal average) pulsed ultrasound with a 1.5 MHz wave frequency, pulsed at 1 kHz for a duration of 20 minutes. For sham treatments, the transducer was applied, but not activated. For intensity investigations, a similar device with variable power output (30, 15, 6 and 2 mW/cm^2) was used.

Immunohistochemistry

10-μm sections of 4% paraformaldehyde-fixed, paraffin-embedded skin were immunostained with antibodies against FSP1 and macrophage marker, F4/80 (Abcam) and fibronectin (Millipore). Primary antibody binding was visualized with biotinylated secondary antibody, ABC-HRP conjugate and 3,3-diaminobenzidine developing reagent (Vector Laboratories), and sections counterstained with haematoxylin (Sigma).

Cell culture

Tiam1 wild-type and knockout MEFs were cultured at 37°C in DMEM, 10% fetal bovine serum, 4.5 g/l glucose, 2 mM L-glutamine. Immortalized wild-type and syndecan-4-knockout MEFs, generated as previously described (Bass 2007), were cultured at 33°C to preserve temperature dependent expression of large T antigen driven immortality in DMEM, 10% fetal bovine serum, 4.5 g/l glucose, 2 mM L-glutamine and 20 U/ml IFNγ (Sigma). Chronic wound fibroblasts were obtained from tissue biopsies after approval from the Local Research Ethics Committee (09/WSE03/19) and written informed consent from patients with non-healing, chronic venous leg ulcers attending the Wound Healing Clinic at the University Hospital of Wales, Cardiff. Only patients with wounds that failed to respond to conventional treatment regimes after 2 months were used in the study. Chronic wound fibroblasts were isolated and cultured as described previously (Cook *et al.*, 2000). Telomerase-immortalized human fibroblasts were cultured at 37°C in DME, 15% fetal bovine serum, 4.5 g/l glucose, 25 mM HEPES and 2 mM L-glutamine.

siRNA duplexes with ON TARGET™ modification, targeting the sense strand of mouse Vav2 (CAAAUGGGCGGAUCGGUUGUU) and Dock180 (GAUAUUGAUCGGUUACAUAUU), were purchased from Dharmacon (Thermo Fisher Scientific). For knockdown of CamKII, both A and B subunits were targeted by esiRNA (Sigma). siRNAs were transfected into immortalized MEFs over two rounds using Dharmafect2 reagent (Thermo Fisher Scientific). Expression of target proteins in comparison with mock-transfected cells was tested by Western blotting.

Migration analysis

CDM was prepared as described previously by culturing confluent fibroblasts for 10 days before removing the fibroblasts by NH4OH lysis (Bass *et al.*, 2007). For migration, cells were seeded at 5000 cells/ml and allowed to spread for 4 hours before capturing time-lapse images at 10-minute intervals for 16 hours on a Leica AS MDW microscope using a 5x NA 0.15 Fluotar objective and Roper CCD camera. The migration paths of all non-dividing,

non-clustered cells were tracked using ImageJ software. Persistence was calculated by dividing linear displacement of a cell over 10 hours by the total distance migrated.

Cell spreading for biochemical assays

GTPase and PAK-activation assays were conducted on surfaces coated with a recombinant fibronectin polypeptide encompassing type III repeats 6-10 that comprises the $\alpha_5\beta_1$-integrin ligand (Bass *et al.*, 2007). 6-well or 96-well tissue culture-treated plastic dishes (Corning BV) were coated overnight at 4°C with 20 μg/ml 50K in Dulbecco's PBS containing calcium and magnesium (Sigma), and blocked with 10 mg/ml heat-denatured BSA. To prevent *de novo* synthesis of ECM and other syndecan-4 ligands, cells were treated with 25 μg/ml cycloheximide (Sigma) for 2 hours prior to the assay. Cells were spread on the 50K-coated plates for 2 hours in DMEM, 4.5 g/l glucose, 25 mM HEPES, 25 μg/ml cycloheximide. Spread cells were stimulated with ultrasound (30 $mWcm^{-2}$, 1.5 MHz wave frequency, 1 kHz pulse frequency), or the syndecan-4-binding fragment of fibronectin (Bass *et al.*, 2007). Where appropriate, pharmacological inhibitors were included throughout spreading and stimulation: 20μM KN93 (Calbiochem), 200 nM Thapsigargin (Calbiochem), 50μM BAPTA, 50μM BAPTA-AM (Life Technologies).

GTPase activity assays

Cells were lysed in 20 mM HEPES (pH 7.4), 10% (v/v) glycerol, 140 mM NaCl, 1% (v/v) Nonidet P-40, 0.5% (w/v) sodium deoxycholate, 4 mM EGTA, 4 mM EDTA, cOmplete protease inhibitor. GST-PAK-CRIB-loaded agarose beads were incubated with the lysates for 1 hour and then washed 3 times with lysis buffer. Bound proteins were blotted for Rac1 or Cdc42 (BD Transduction Labs).

In-cell ELISA

Cells fixed in 4% PFA were permeablized with 0.1% Triton X-100 in TBS and blocked to reduce non-specific binding (Sigma casein block in TBS). Anti-phospho-Serine141 PAK1/2/3 antibody (Life Technologies, diluted 1:800 in TBS-block was applied to each well overnight. Cells were washed in TBS containing 0.1% Tween-20 and primary antibody binding was visualized with Alexa-fluor 800-conjugated anti-rabbit IgG diluted 1:5000 in TBS-block. Wells were washed of unbound secondary antibody and the plates scanned quantified (Odyssey fluorescent detection system, LI-COR Biosciences).

Supplementary Material

Refer to Web version on PubMed Central for supplementary material.

Acknowledgements

This work was supported by Wellcome Trust grant 088419 and sponsorship by Bioventus LLC to MDB. Microscopes were part of the Wolfson Bioimaging Facility and Mass Spectrometry conducted by the Proteomics Facility, University of Bristol.

Europe PMC Funders Author Manuscripts

References

Altomare M, Nascimento AP, Romana-Souza B, et al. Ultrasound accelerates healing of normal wounds but not of ischemic ones. Wound Repair Regen. 2009; 17:825–31. [PubMed: 19821959]

Angle SR, Sena K, Sumner DR, et al. Osteogenic differentiation of rat bone marrow stromal cells by various intensities of low-intensity pulsed ultrasound. Ultrasonics. 2011; 51:281–8. [PubMed: 20965537]

Ansell DM, Holden KA, Hardman MJ. Animal models of wound repair: Are they cutting it? Exp Dermatol. 2012; 21:581–5. [PubMed: 22775993]

Atkinson MA, Leiter EH. The NOD mouse model of type 1 diabetes: as good as it gets? Nat Med. 1999; 5:601–4. [PubMed: 10371488]

Azuma Y, Ito M, Harada Y, et al. Low-intensity pulsed ultrasound accelerates rat femoral fracture healing by acting on the various cellular reactions in the fracture callus. J Bone Miner Res. 2001; 16:671–80. [PubMed: 11315994]

Bass MD, Roach KA, Morgan MR, et al. Syndecan-4-dependent Rac1 regulation determines directional migration in response to the extracellular matrix. J Cell Biol. 2007; 177:527–38. [PubMed: 17485492]

Claes L, Willie B. The enhancement of bone regeneration by ultrasound. Prog Biophys Mol Biol. 2007; 93:384–98. [PubMed: 16934857]

Cook H, Davies KJ, Harding KG, et al. Defective extracellular matrix reorganization by chronic wound fibroblasts is associated with alterations in TIMP-1, TIMP-2, and MMP-2 activity. J Invest Dermatol. 2000; 115:225–33. [PubMed: 10951240]

Coords M, Breitbart E, Paglia D, et al. The effects of low-intensity pulsed ultrasound upon diabetic fracture healing. J Orthop Res. 2011; 29:181–8. [PubMed: 20886648]

Duarte LR. The stimulation of bone growth by ultrasound. Arch Orthop Trauma Surg. 1983; 101:153–9. [PubMed: 6870502]

Echtermeyer F, Streit M, Wilcox-Adelman S, et al. Delayed wound repair and impaired angiogenesis in mice lacking syndecan-4. J Clin Invest. 2001; 107:R9–R14. [PubMed: 11160142]

Emami A, Petren-Mallmin M, Larsson S. No effect of low-intensity ultrasound on healing time of intramedullary fixed tibial fractures. Journal of orthopaedic trauma. 1999; 13:252–7. [PubMed: 10342350]

Falanga V. Wound healing and its impairment in the diabetic foot. Lancet. 2005; 366:1736–43. [PubMed: 16291068]

Fleming IN, Elliott CM, Buchanan FG, et al. Ca2+/calmodulin-dependent protein kinase II regulates Tiam1 by reversible protein phosphorylation. J Biol Chem. 1999; 274:12753–8. [PubMed: 10212259]

Frankel VH, Mizuho K. Management of non-union with pulsed low-intensity ultrasound therapy--international results. Surg Technol Int. 2002; 10:195–200. [PubMed: 12384881]

Galiano, RD.; Mustoe, TA. Chapter 3: Wound Care. Grabb and Smith's Plastic Surgery. 6th ed. Thorne, CH., editor. Lippincott Williams and Wilkins; 2007. p. 23-32.

Harding KG, Moore K, Phillips TJ. Wound chronicity and fibroblast senescence--implications for treatment. Int Wound J. 2005; 2:364–8. [PubMed: 16618323]

Hassanain HH, Irshaid F, Wisel S, et al. Smooth muscle cell expression of a constitutive active form of human Rac 1 accelerates cutaneous wound repair. Surgery. 2005; 137:92–101. [PubMed: 15614286]

Heckman JD, Ryaby JP, McCabe J, et al. Acceleration of tibial fracture-healing by non-invasive, low-intensity pulsed ultrasound. J Bone Joint Surg Am. 1994; 76:26–34. [PubMed: 8288661]

Ishiguro K, Kadomatsu K, Kojima T, et al. Syndecan-4 deficiency impairs focal adhesion formation only under restricted conditions. J Biol Chem. 2000; 275:5249–52. [PubMed: 10681494]

Kristiansen TK, Ryaby JP, McCabe J, et al. Accelerated healing of distal radial fractures with the use of specific, low-intensity ultrasound. A multicenter, prospective, randomized, double-blind, placebo-controlled study. J Bone Joint Surg Am. 1997; 79:961–73. [PubMed: 9234872]

Kwon AH, Qiu Z, Hirao Y. Topical application of plasma fibronectin in full-thickness skin wound healing in rats. Exp Biol Med. 2007; 232:935–41.

Leung KS, Cheung WH, Zhang C, et al. Low intensity pulsed ultrasound stimulates osteogenic activity of human periosteal cells. Clin Orthop Relat Res. 2004:253–9. [PubMed: 15043127]

Liu S, Kapoor M, Leask A. Rac1 expression by fibroblasts is required for tissue repair in vivo. Am J Pathol. 2009; 174:1847–56. [PubMed: 19349358]

Mahoney CM, Morgan MR, Harrison A, et al. Therapeutic ultrasound bypasses canonical syndecan-4 signaling to activate rac1. J Biol Chem. 2009; 284:8898–909. [PubMed: 19147498]

Menke NB, Ward KR, Witten TM, et al. Impaired wound healing. Clin Dermatol. 2007; 25:19–25. [PubMed: 17276197]

Naruse K, Sekiya H, Harada Y, et al. Prolonged endochondral bone healing in senescence is shortened by low-intensity pulsed ultrasound in a manner dependent on COX-2. Ultrasound Med Biol. 2010; 36:1098–108. [PubMed: 20620697]

Pounder NM, Harrison AJ. Low intensity pulsed ultrasound for fracture healing: a review of the clinical evidence and the associated biological mechanism of action. Ultrasonics. 2008; 48:330–8. [PubMed: 18486959]

Raftopoulou M, Hall A. Cell migration: Rho GTPases lead the way. Dev Biol. 2004; 265:23–32. [PubMed: 14697350]

Sen CK, Gordillo GM, Roy S, et al. Human skin wounds: a major and snowballing threat to public health and the economy. Wound Repair Regen. 2009; 17:763–71. [PubMed: 19903300]

Shaw TJ, Martin P. Wound repair at a glance. J Cell Sci. 2009; 122:3209–13. [PubMed: 19726630]

Swulius MT, Waxham MN. Ca(2+)/calmodulin-dependent protein kinases. Cell Mol Life Sci. 2008; 65:2637–57. [PubMed: 18463790]

Tang CH, Yang RS, Huang TH, et al. Ultrasound stimulates cyclooxygenase-2 expression and increases bone formation through integrin, focal adhesion kinase, phosphatidylinositol 3-kinase, and Akt pathway in osteoblasts. Mol Pharmacol. 2006; 69:2047–57. [PubMed: 16540596]

Wall IB, Moseley R, Baird DM, et al. Fibroblast dysfunction is a key factor in the non-healing of chronic venous leg ulcers. J Invest Dermatol. 2008; 128:2526–40. [PubMed: 18449211]

Woodley DT, Remington J, Huang Y, et al. Intravenously injected human fibroblasts home to skin wounds, deliver type VII collagen, and promote wound healing. Mol Ther. 2007; 15:628–35. [PubMed: 17245357]

Zahorec P, Koller J, Danisovic L, et al. Mesenchymal stem cells for chronic wounds therapy. Cell Tissue Bank. 2014

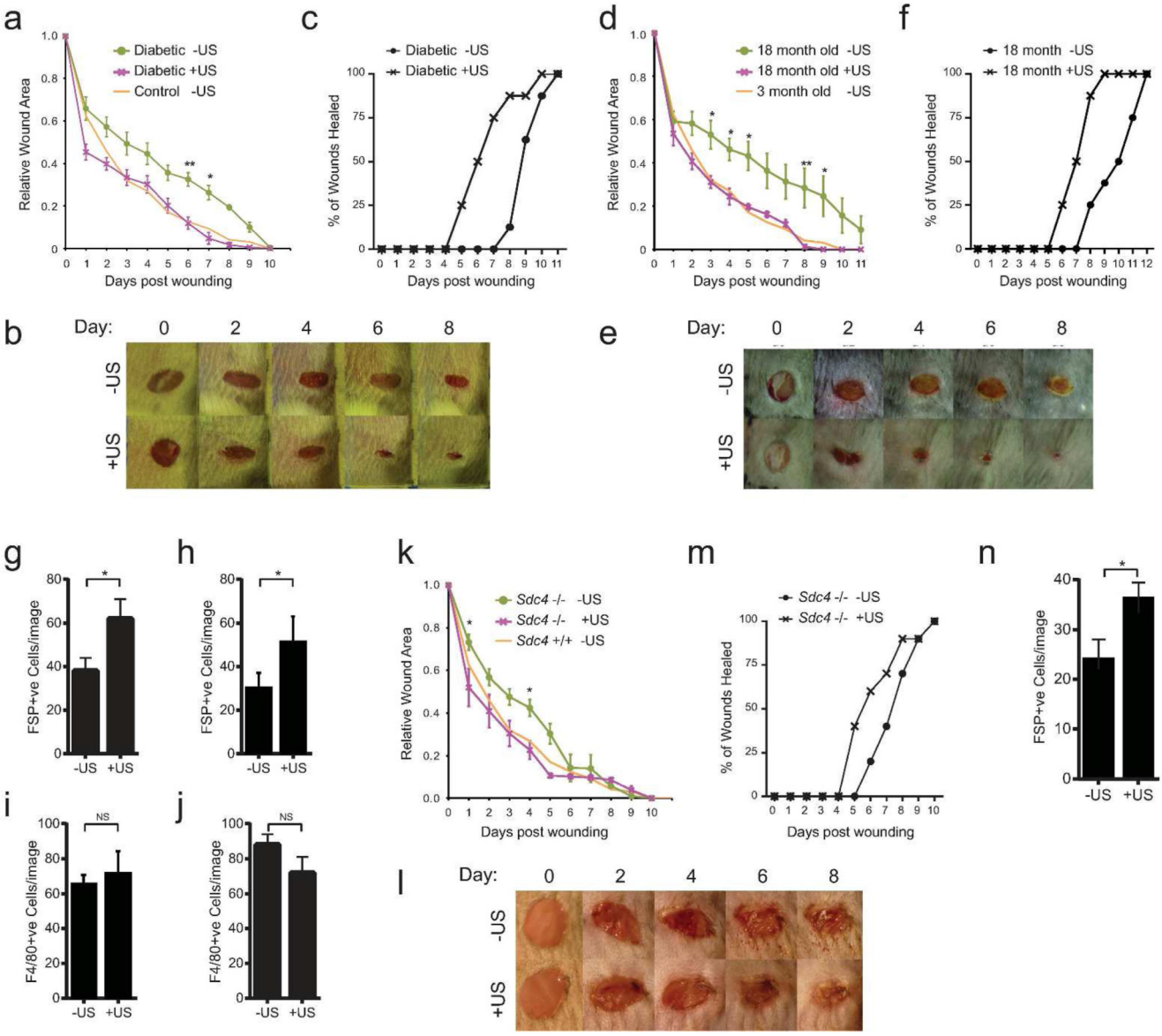

Fig. 1. Rescue of defective healing in mouse models.

4-mm full-thickness punch wounds on mice with characterized healing defects or matched controls were subjected to daily ultrasound or sham treatments and wound closure was recorded. (A-C,G+I) Diabetic (NOD). (D-F,H+J) 18-month and 3-month old. (K-N) *Sdc4* -/- and +/+. (A-B,D-E,K-L) Daily macroscopic images and measurements of wound area. (C,F,M) Animals scored for loss of the scab as an indicator of wound resolution. (G-J,N) Skin sections stained for fibroblast-specific protein (FSP) and macrophages (F4/80) at 72 hours post-wounding, and scored for fibroblast or macrophage number per field of view. Example images shown in figure S1+S2A-B+E-F). Data are representative of 12 wounds in 6 mice per condition. Error bars indicate s.e.m. Significance tested by Students T-test, *=p<0.05, **=p<0.005.

Europe PMC Funders Author Manuscripts

Europe PMC Funders Author Manuscripts

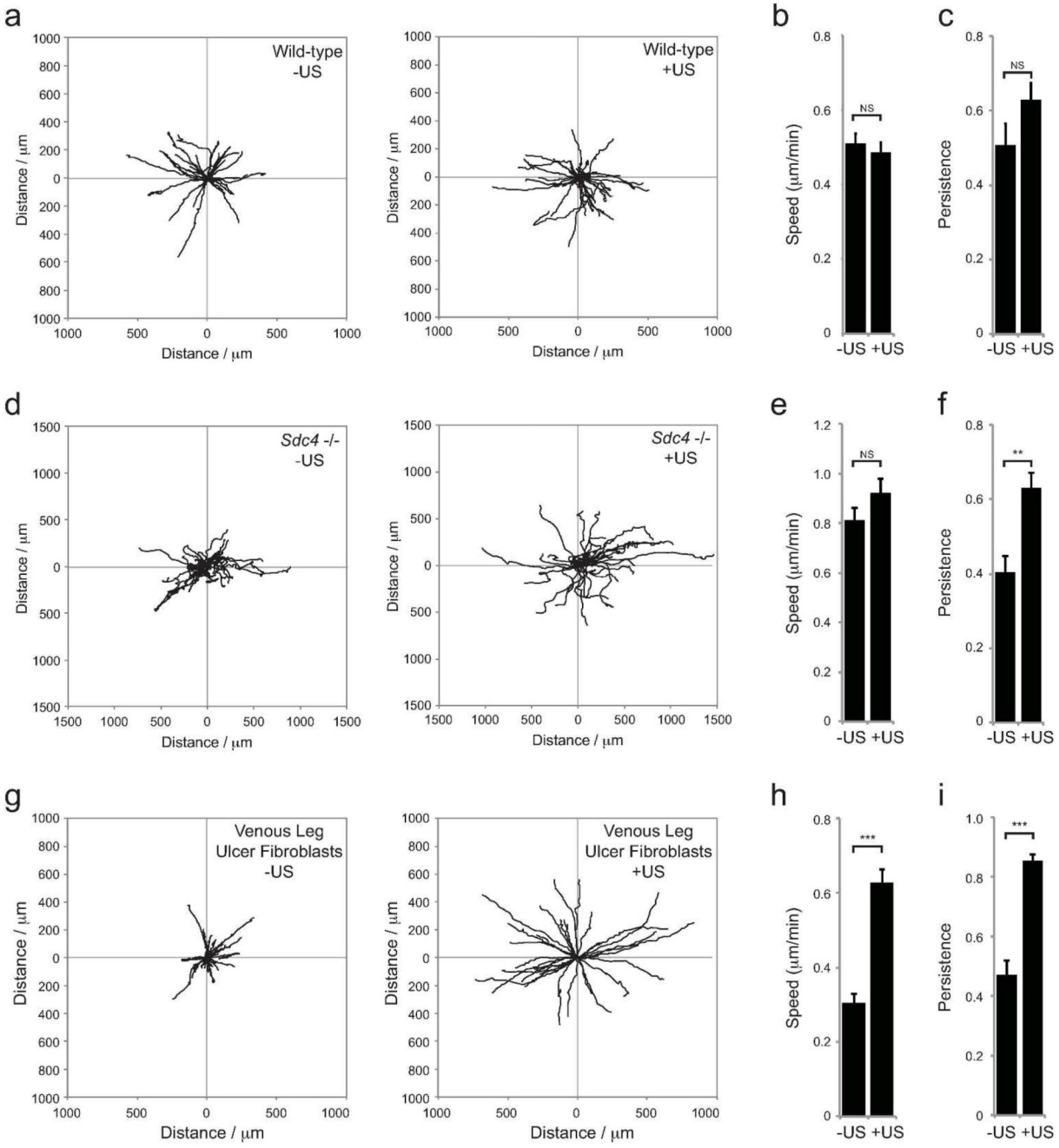

Fig. 2. Restoration of defective fibroblast migration.

Sham or ultrasound-treated wild-type (A-C), *Sdc4* -/- (D-F), or chronic venous leg ulcer fibroblasts (G-I) were seeded onto fibrous cell derived matrix and migration tracked over 16 hours. (A, D, G) Example tracks. (B, E, H) Average migration speed (total distance moved/ time). (C, F, I) Average persistence of migration (total displacement/total distance moved, so that for perfect linear migration, persistence =1). Error bars indicate s.e.m., n=60 per condition. Significance tested by Kruskal-Wallis test, **=p<0.005, ***=p<0.0005.

Europe PMC Funders Author Manuscripts

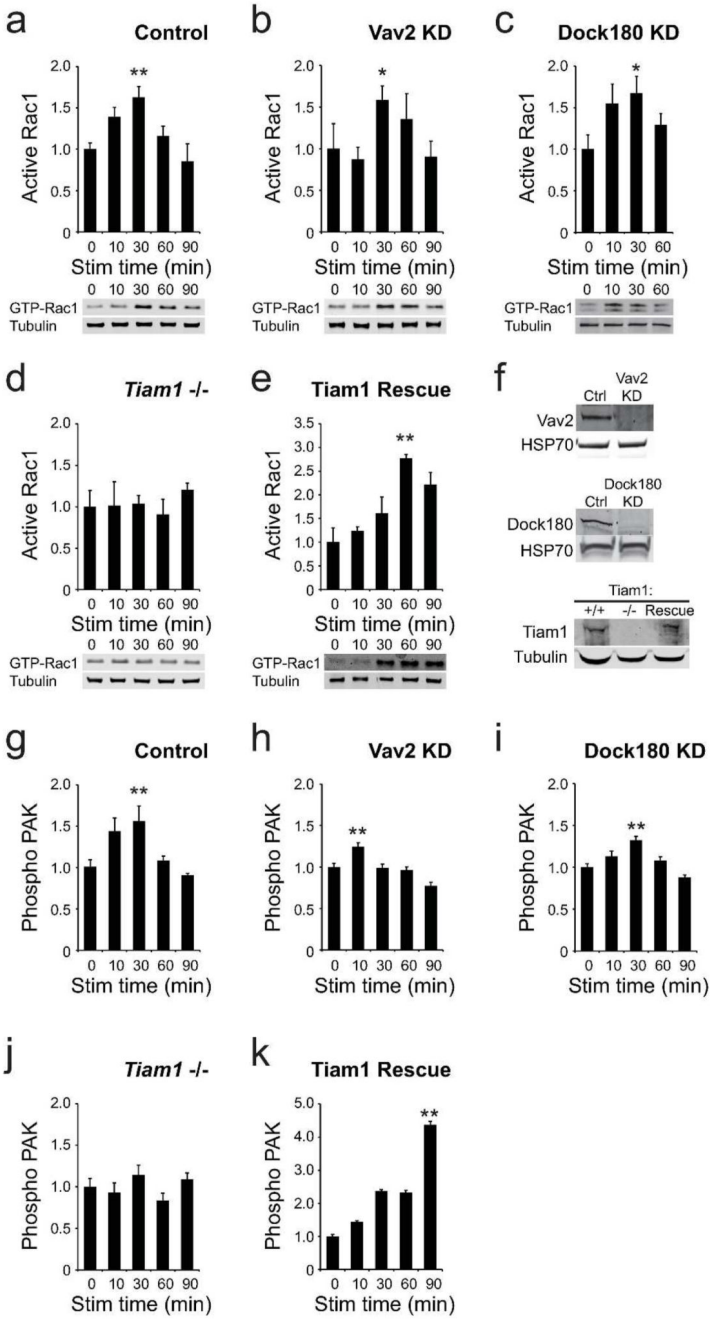

Fig. 3. Tiam1 mediates Rac1 activation in response to ultrasound.

MEFs were spread on the integrin-binding fragment of fibronectin, stimulated with ultrasound and analyzed at the appropriate time from the start of stimulation. (A-E) Rac1 activity measured by effector pulldown assay, n=5 per condition (F) Expression of candidate GEFs in the corresponding experiments. (G-K) PAK phosphorylation measured by in-cell ELISA, n=12 per condition. Error bars indicate s.e.m. Significance tested by ANOVA, *=$p<0.05$, **=$p<0.005$.

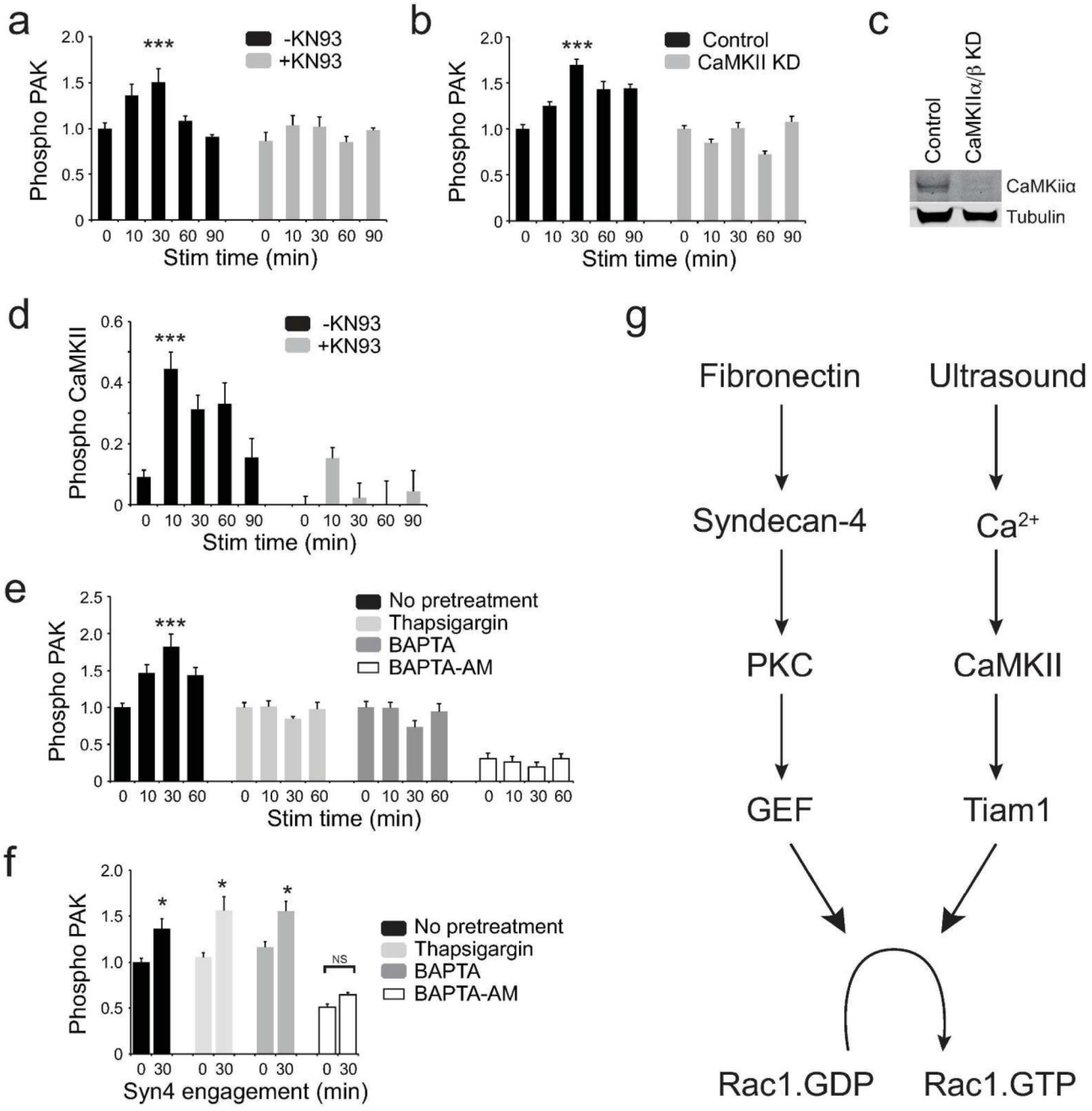

Fig. 4. CamKII mediates Rac1 activation in response to ultrasound.

Inhibitor-treated MEFs were stimulated with ultrasound and analyzed by in-cell ELISA. (A-C) PAK activation following treatment with vehicle or 20 μM KN93 (CamKII inhibitor), n=16 (A), or knockdown of CamKII, n=24 (B). Confirmation of CamKII knockdown (C). (D) Ultrasound induces autophoshorylation of CamKII and can be blocked by KN93, n=16. (E-F) Treatment with 200 nM thapsigargin, 50μM BAPTA, or 50μM BAPTA-AM blocks PAK phosphorylation in response to ultrasound, n=5 (E), but thapsigargin and BAPTA do not block PAK phosphorylation in response to the syndecan-4-binding fragment of

fibronectin, n=4 (F). (G) Mechanical (ultrasound) and chemical (fibronectin) stimuli activate Rac1 by different pathways. Error bars indicate s.e.m. Significance tested by ANOVA, *=p<0.05, ***=p<0.0005.

Europe PMC Funders Author Manuscripts

Europe PMC Funders Author Manuscripts

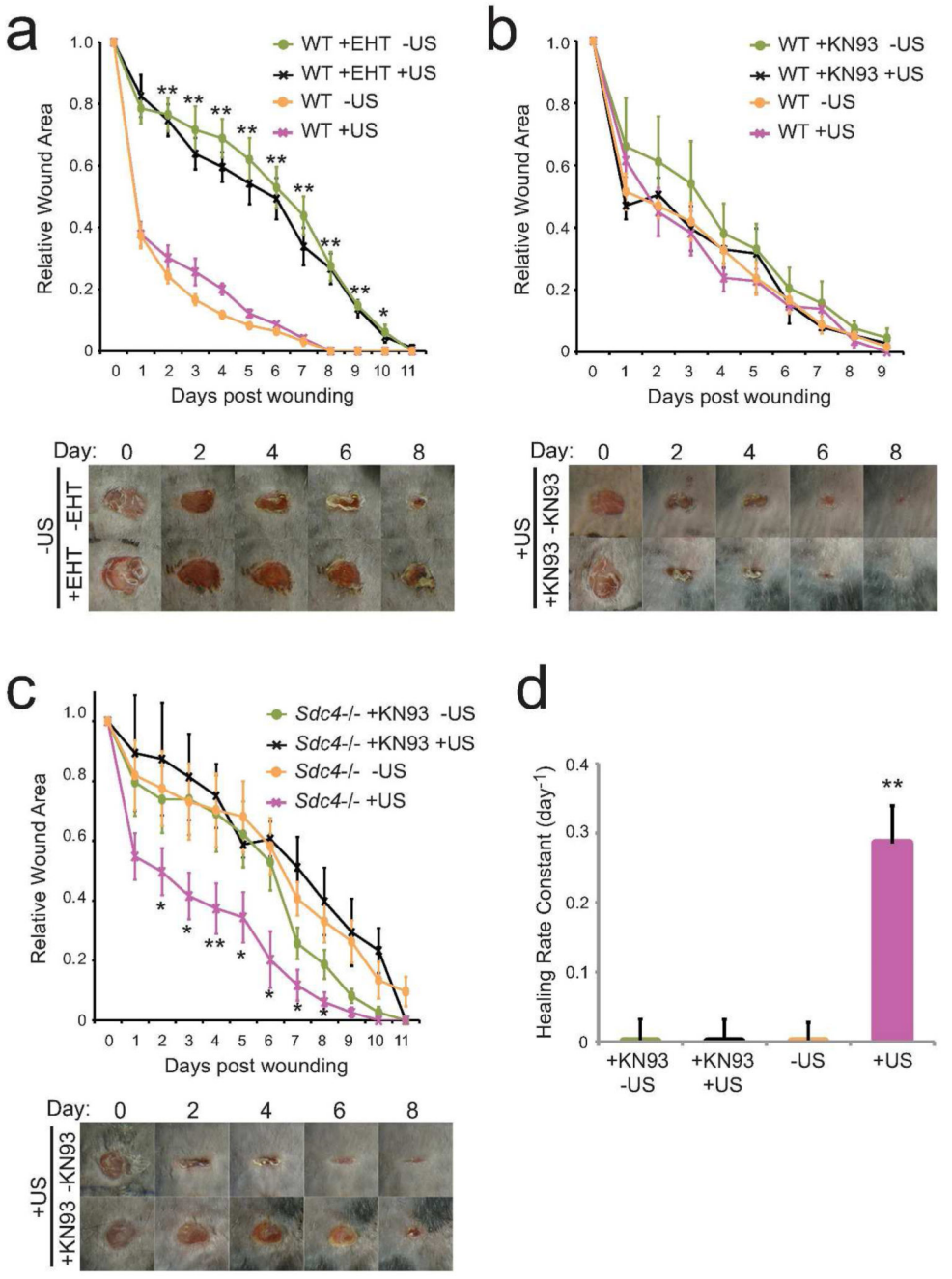

Fig. 5. Independent Rac1 activation pathways drive wound closure in mice.

4-mm full-thickness punch wounds on wild-type (A+B) or *Sdc4* -/- (C+D) mice were treated with vehicle of pharmacological inhibitor, 50μM EHT 1864 (A) or 20μM KN93 (B-D) in pluronic gel. Wounds were subjected to daily ultrasound or sham treatments and wound closure was recorded. (D) Rate constants of curves depicted in (C). Data are representative of 6 mice per condition. Error bars indicate s.e.m. (A) Significance of + vs − EHT tested by

paired T-test, (C) Significance of +KN93+US vs +US tested by paired T-test, *=p<0.05, **=p<0.005.

Europe PMC Funders Author Manuscripts